INTERNATIONAL JOURNAL OF ENERGY RESEARCH
Int. J. Energy Res. 2007; **31**:119–134
Published online 9 August 2006 in Wiley InterScience
(www.interscience.wiley.com) DOI: 10.1002/er.1231

Performance characteristics and modelling of a micro gas turbine for their integration with thermally activated cooling technologies

Adrián Vidal[1], Joan Carles Bruno[2], Roberto Best[1] and Alberto Coronas[2,*,†]

[1] *Centro de Investigación en Energía-UNAM, Posgrado en Ingeniería-Energía, Privada Xochicalco, s/n, col. Centro, 62580, Temixco, Morelos, Mexico*
[2] *CREVER-Universitat Rovira i Virgili, Autovia de Salou, s/n, 43006 Tarragona, Spain*

SUMMARY

We have developed a simple model of a micro gas turbine system operating at high ambient temperatures and characterized its performance with a view to integrating this system with thermally activated cooling technologies. To develop and validate this model, we used experimental data from the micro gas turbine test facility of the CREVER research centre. The microturbine components were modelled and the thermodynamic properties of air and combustion gases were estimated using a commercial process simulator. Important information such as net output power, microturbine fuel consumption and exhaust gas mass flow rate can be obtained with the empirical correlations we have developed in this study. This information can be useful for design exhaust gas fired absorption chillers. Copyright © 2006 John Wiley & Sons, Ltd.

KEY WORDS: modelling; micro gas turbine; cogeneration; waste heat; cooling

1. BACKGROUND AND OBJECTIVES

For building applications in which energy demand is closely related to climatic conditions, adding an absorption chiller to a micro gas turbine based cogeneration system is a good way to increase cost efficiency. At high ambient temperatures, however, the performance of the micro gas turbine is somewhat degraded. Manufacturers offer only limited information on microturbine derated performance characteristics at off-design conditions (power capacity,

*Correspondence to: Alberto Coronas, CREVER-Universitat Rovira i Virgili, Autovia de Salou, s/n, 43006 Tarragona, Spain.
† E-mail: alberto.coronas@urv.net

Contract/grant sponsor: Posgrado de Ingeniería, UNAM
Contract/grant sponsor: Government of Catalonia
Contract/grant sponsor: CONACYT; contract/grant number: 44764-Y

Received 16 November 2005
Revised 19 May 2006
Accepted 29 May 2006

exhaust gas temperature and flow rate, etc.). This type of information is important for designing exhaust gas fired absorption chillers characterized by a higher driven temperature and efficiency than hot-water driven systems.

Micro gas turbines (MGT) for on-site small-scale energy production provide a great opportunity for saving primary energy and reducing pollutant and greenhouse gas emissions, mainly because waste heat can be easily recovered from the exhaust gas, especially for high-efficiency air conditioning thermally activated technologies, and because they can use low heating value gases such as digester gas. There is no clear definition of the size of microturbines, but micro gas turbines can be defined as small high-speed turbo-alternators of up to 200 kWe. They operate as a Brayton cycle that comprises a centrifugal compressor, a regenerator, a combustion chamber and a radial turbine connected to a permanent magnet alternator rotor. Their main features are that the high-speed generator is directly coupled to the turbine rotor and they use power electronics instead of a gearbox and a conventional generator to adapt the power produced to the grid power quality (Pilavachi, 2002; Bullin, 2002).

In a typical micro gas turbine configuration, as shown in Figure 1, the combustion air is first filtered and used to cool the electric generator (EG) before it enters the compressor (AC), where it is pressurized and forced into the cold side of the regenerator (RE). In the regenerator, the turbine exhaust heat (6) is used to preheat the combustion air (2) to reduce the amount of fuel required. In the combustion chamber (CC), the heated air is mixed with fuel (4) and burned. The hot exhaust gas (5) expands through the turbine (GT) that drives the compressor and the electric generator and finally enters the regenerator.

The need to better understand the performance of this new distributed generation technology has led to an increase in research and demonstration projects with microturbines. There are a few recent references in the literature on the performance of microturbines and the emission levels obtained from experimental tests on microturbines e.g. Fairchild *et al.* (2001), Gomes *et al.* (2004) and Bruno *et al.* (2004). Other research on micro gas turbines has focused only on modelling

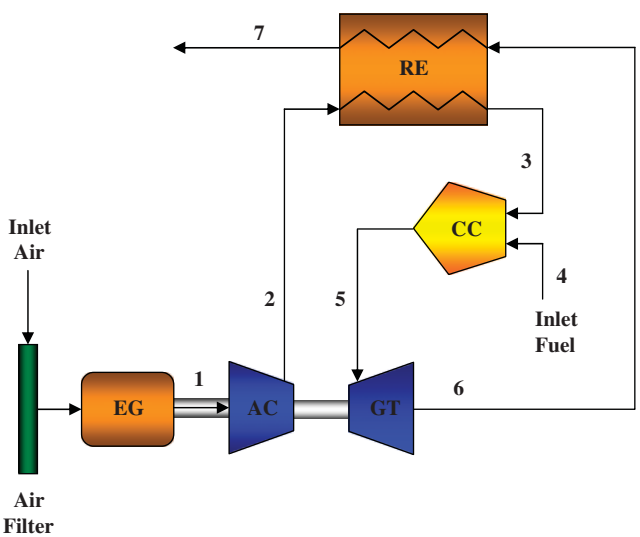

Figure 1. Schematic diagram of the modelled micro gas turbine cycle. EG = Electric Generator, AC = Air Compressor, GT = Gas Turbine, CC = Combustion Chamber, RE = Regenerator.

DOI: 10.1002/er

aspects such as part load behaviour (Zhang and Cai, 2002; Wang *et al.*, 2004). Campanari *et al.* (2002) modelled the microturbine using parameters from the limited data in the open literature.

As micro gas turbine power is not very efficient, it is important to recover the maximum useful waste heat. Bouvy *et al.* (2004) presented the case of a 50 kWe micro gas turbine with a two-stage heat recovery system at two different temperatures. Also, adding an absorption chiller to a micro gas turbine based cogeneration system for building applications, where energy demand is closely related to climate conditions, is known to be a good way to increase the economic performance of the system. In this way, the number of running hours is extended to periods of high ambient temperatures in summer, when the microturbine waste heat is not required, though there is a demand for cooling. Several references have appeared in the literature on the integration of microturbines and absorption chillers due to their energy saving potential. The most conventional approach is to use the exhaust heat to produce hot water to drive the chiller. See, for example, Pinto and Bazzo (2003), who presented a preliminary thermoeconomic analysis for a microturbine of 30 kWe and a hot-water-driven absorption chiller with a cooling capacity of 29.8 kW and a COP of 0.65. Banetta *et al.* (2001) presented an experimental facility consisting of a microturbine and a hot-water-driven absorption chiller/heater.

The driving of absorption chillers directly by exhaust gas has also been studied, though to a lesser extent. Hwang (2004) studied the theoretical performance of a direct exhaust gas driven water/LiBr system to provide subcooling to a condenser in a compression refrigeration system and air precooling to a micro gas turbine. In these cases, the chilled water temperature was set rather high (at 10 °C) in order to use an air-cooled absorption chiller. Bruno *et al.* (2005) explored the benefits of directly using the exhaust gas in an absorption chiller with supplementary post-combustion to increase the cooling capacity and system flexibility to match the cooling production and demand independently from the power production at any time. We should point out that several absorption chillers, specially designed for their coupling with specific microturbines (UTC Power, 2005; Elliott Energy Systems, 2003) or adapted to regenerative microturbines characteristics (Broad Air Conditioning, 2005), are currently starting its commercialization.

Previous examples of the integration of microturbines with absorption chillers have demonstrated the great interest in improving these types of applications, which can be extended to the integration of other thermally activated cooling technologies such as vapour jet refrigeration (Invernizzi and Iora, 2005) and solid wheel desiccant systems (Cowie *et al.*, 2003). Obviously these cooling technologies are operated when ambient temperatures are high. At high ambient temperatures, however, the micro gas turbine performance is degraded by a certain amount. Ho *et al.* (2004) reported the performance of a microturbine and a hot-water-driven water/LiBr chiller. Although not clearly stated in that paper, the system offered poor performance (a COP of between 0.5 and 0.58), probably because of very high ambient temperatures that also reduced the microturbine efficiency to only 21%. Microturbine manufacturers provide only limited information about microturbine derated performance characteristics at off-design conditions. This type of information is important for designing integrated microturbine and absorption chillers, which are obviously in service at high ambient temperatures.

In this paper we characterize the performance of a micro gas turbine that describes the behaviour of a micro gas turbine operating at high ambient temperatures and develop a simple model using a commercial process simulator. The micro gas turbine model was developed and validated using experimental data from the test facility of the CREVER research centre (Bruno *et al.*, 2004).

DOI: 10.1002/er

Our results are relevant for the integration of micro gas turbines with thermally activated technologies, i.e. in applications in which the ambient temperature is relatively high, because important information as net output power, microturbine fuel consumption and exhaust gas mass flow rate can be estimated with the empirical correlations obtained in this study. As well as ambient temperature, another aspect to be considered is the drop in pressure caused by each cooling thermally activated technology. The drop in pressure in such cases has been shown to be a significant issue (Bouvy *et al*., 2004). The development of compact and efficient exhaust gas driven generators for absorption chillers must also be correctly addressed (Sang *et al*., 2005; Kren *et al*., 2005).

2. EXPERIMENTAL FACILITIES

Our experimental data were obtained from the micro gas turbine test facility of the CREVER research centre (Tarragona, Spain). The MGT can be fuelled by natural gas or by propane. For the results shown here we used propane. The microturbine was a Capstone C30 model of 30 kWe operating as a high-pressure system, plus a gas-water heat exchanger to produce hot water. The propane supply system comprised a set of propane cylinders that interfaced with the microturbine through a pressure regulator. Figure 2 is a schematic overview of this system. When the micro gas turbine operates with natural gas due to the pressure of the supply line, it operates as a low-pressure system and an integrated natural gas compressor is used. A more detailed description of the test facility was presented in Bruno *et al*. (2004).

All the micro gas turbine external temperatures: ambient air, exhaust gas at the MGT outlet, exhaust gas to the atmosphere, boiler inlet and outlet streams were collected using RTD (PT-100) temperature sensors. Propane gas consumption was measured with both a Mass Flow

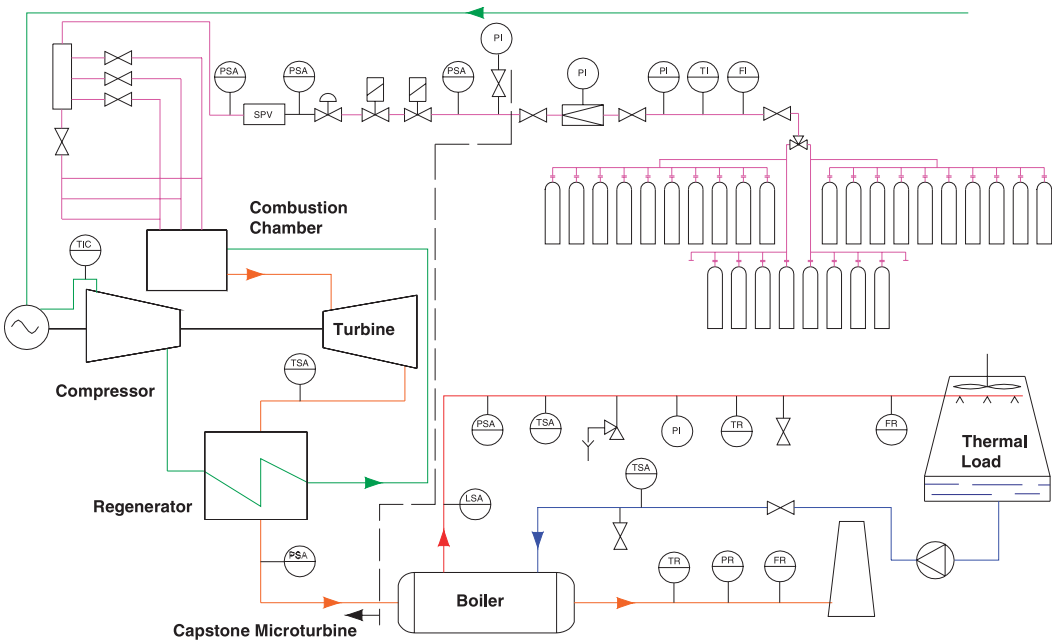

Figure 2. Overview of the micro gas turbine test facility.

DOI: 10.1002/er

Transmitter Multivariable Model Rosemount 3095 MV and an Integral orifice Rosemount Model 1195 as primary element. Exhaust gas flow was measured with a Rosemount Mass Probar Flowmeter with an annubar sensor. All the other variables, such as output power and microturbine internal variables (air temperature at the electric generator output, temperature at the turbine outlet, fuel pressure, etc.) were obtained using the built-in measuring devices provided by the microturbine manufacturer monitored with the Capstone Remote Monitoring System (CRMS) software.

3. MICRO GAS TURBINE PERFORMANCE AT HIGH AMBIENT TEMPERATURES

Like the performance of any other type of gas turbine, the performance of the microturbine is greatly affected by ambient temperature and other factors such as altitude, air intake and drops in exhaust gas pressure. As the ambient temperature increases, the efficiency and output power of the microturbine both decrease. This performance degradation is due to the reduction in the inlet air and fuel mass flow rate as the air density decreases with ambient temperature.

The microturbine electric output power can be selected in two ways:

1. By running the microturbine at a constant output power. In this case, a setpoint for the output power is set at a lower value than the maximum power that can be achieved for a given ambient temperature. Figure 3 represents the output power for the microturbine set to provide 22 kW of electricity and the ambient temperature for reference. The output power is not affected by ambient temperature but the electric efficiency decreases by around 0.5% for a 5 °C increase in ambient temperature (see Figure 4). The LHV used in this calculation for propane was 46 310.22 kJ/kg.
2. By running the microturbine at the maximum output power that can be achieved for the existing ambient temperature. For this case, the setpoint is set at a higher value than the one that can be reached with the existing ambient conditions.

In this study, the microturbine was operated as in point 2 above, i.e. at its maximum power at any time. In this case, the output power follows the same trend as the ambient temperature. The

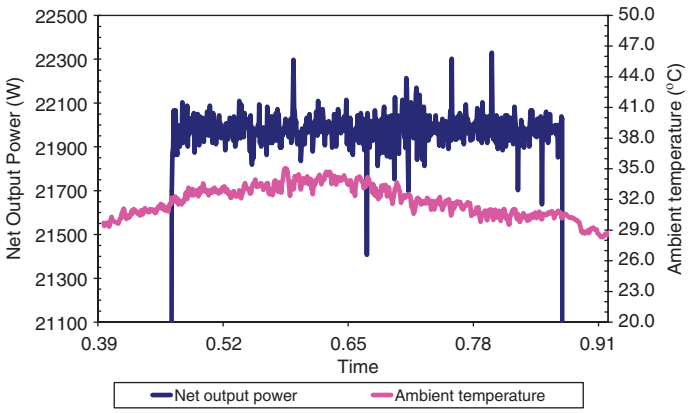

Figure 3. Net output power with the setpoint at 22 kWe.

DOI: 10.1002/er

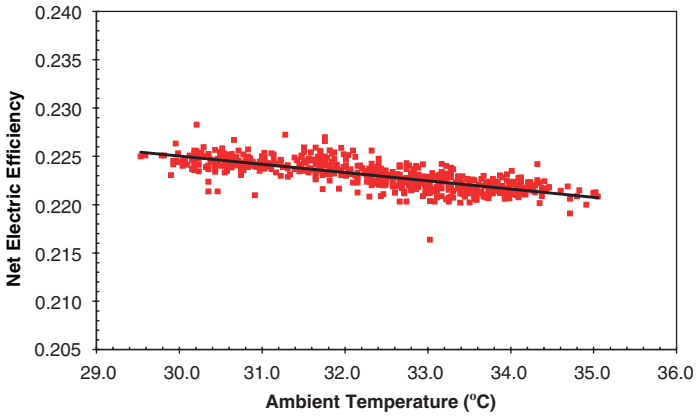

Figure 4. Net electric efficiency for a constant electric output power of 22 kWe.

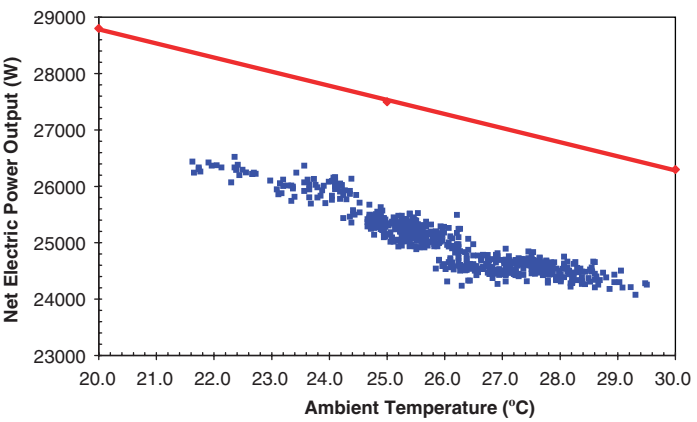

Figure 5. Net electric power output of the microturbine as a function of ambient temperature.

off-design performance of the microturbine was investigated between 21 and 30 °C, which is a typical range of summer temperature in the area of Tarragona (Spain) and is representative of other non-extreme warm Mediterranean areas.

The net electric power of the microturbine at various ambient temperatures is given in Figure 5. The blue dots are experimental data points and the red line is an approximation of the derating data provided by the manufacturer (Capstone, 2001). The difference between these sets of data is mainly due to contributions to the decrease in power other than ambient temperature, e.g. the considerable drop in exhaust pressure caused by the heat recovery heat exchanger and the exhaust stack, plus other minor contributions such as air humidity, dirt in the air inlet filter and the drop in pressure at the air inlet. The effect of altitude is negligible because the microturbine is located almost at sea level. The microturbine is always operated at its maximum capacity, so the above effects are the cause of performance degradation not partial load operation.

The electric efficiency of the microturbine decreases as the ambient temperature increases (see Figure 6). This is an approximate reduction of 0.75% for a change in ambient temperature of

DOI: 10.1002/er

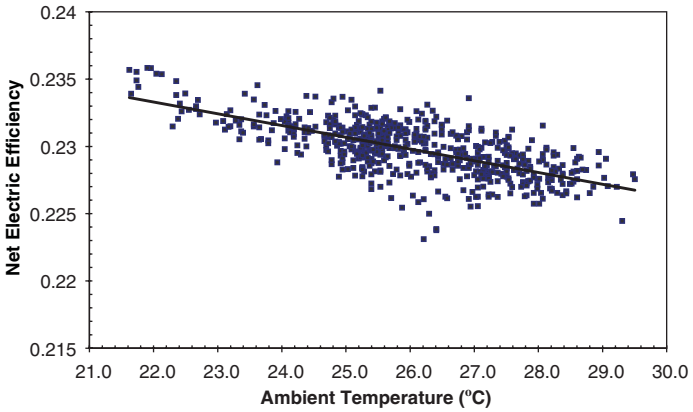

Figure 6. Net electric efficiency for the microturbine operating at its maximum power according to the existing ambient temperature.

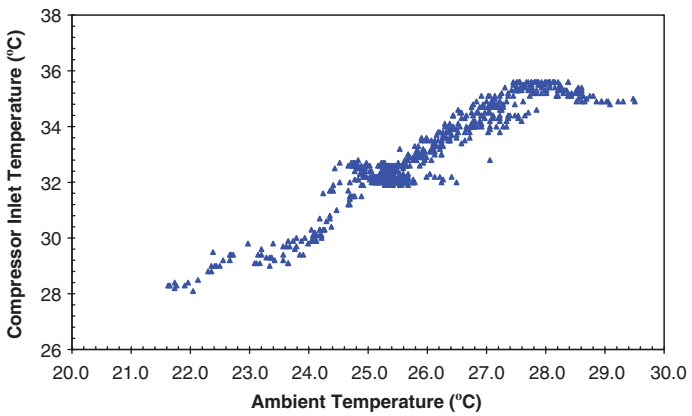

Figure 7. Compressor inlet temperature of the microturbine operating at its maximum power according to the existing ambient temperature.

8 °C, which is very similar to the reduction when operating at a constant power output, i.e. 0.1% per degree of centigrade increase in ambient temperature (Figure 4).

For modelling purposes, it is interesting to analyse how the ambient temperature affects other microturbine operation parameters apart from power output and efficiency. The temperature of the air that finally enters the air compressor is higher than the ambient temperature. Figure 7 shows the relationship between these two temperatures. During the tests, the heat that dissipates from the electric generator to the air is almost constant, so the compressor inlet temperature increases by 1°C for each 1°C increase in ambient temperature. The compressor inlet temperature is roughly 6–7°C higher than the ambient temperature when working at an electric load above 18 kWe (see Figure 7).

The Turbine Exit Temperature (TET) is kept constant at 594 °C by the microturbine control system. This is the minimum temperature for the turbine outlet when it is operated at full load at any given ambient temperature. For a given electric output below the microturbine maximum

DOI: 10.1002/er

capacity, the TET increases as the ambient temperature decreases, so the output power remains constant. In this study, as the turbine exit temperature is constant, since the microturbine is working at the maximum capacity permitted by the existing ambient conditions, the outlet exhaust gas temperature to the waste heat exchanger boiler is also almost constant at 290 °C. In other cases, when the microturbine is working at partial load, the exhaust gas temperature to the boiler decreases as the electric load decreases and follows the same trend as the ambient temperature.

The shaft rotation speed is not only a function of the electric load but also of the ambient temperature. Whenever one of these two parameters increases, the speed also increases to a maximum value of around 96 000 rpm. Note that the maximum output power is not limited by this maximum speed but by the minimum turbine exit temperature (594 °C).

4. MODELLING

The micro gas turbine model was carried out using the Aspen Plus process simulator (Aspen Plus, 2004). This is a process modelling software that is suitable for a variety of steady state modelling applications. The Aspen Plus system is based on 'blocks', corresponding to unit operations, through which most industrial operations can be simulated. By interconnecting the blocks using material, work and heat streams, a complete process flowsheet can be constructed. Aspen Plus includes several databases containing physical, chemical and thermodynamic data for a wide range of chemical compounds, plus a selection of thermodynamic models for accurately simulating any chemical system. Simulation is performed by specifying: (1) the flow rates, compositions and operating conditions of some streams; (2) the operating conditions of the blocks used in the process, e.g. temperature, pressure and number of stages; and (3) the heat and/or work inputs into the process. Using these data, Aspen Plus calculates the flow rates, compositions and state conditions of all outlet material streams, as well as the heat and work output of all outlet heat and work streams. The resulting reports of blocks can be modified to meet user-specific requirements by inserting a Fortran statement or Excel spreadsheet calculations into the flowsheet computation. In addition to these advantages, the main reason for modelling the microturbine with this software is that in future the model can be used for optimization of micro gas turbine based cogeneration plants, polygeneration systems, etc. The user can introduce specific or complex devices into Aspen software by the User Model option, which consists of subroutines that use programming languages such as Fortran. The PR–BM (Peng–Robinson with Boston–Mathias alpha function) equation of state was selected for the micro gas turbine model, since it is one of the physical property methods recommended for combustion (Aspen Plus, 2003). This equation of state produced good results with respect to the experimental data. However, there was just a slight difference between these results and those obtained with the SYSOP0 method based on the Ideal Gas/Raoult's Law method.

The blocks that comprise the microturbine are modelled as follows:

Air compressor: This device is used to compress the air to the pressure required in the combustion chamber. The compressor is simulated using the *COMPR* block in Aspen Plus by introducing the concept of isentropic efficiency, which is defined as

$$\eta_{\text{isen}} = \frac{\dot{W}_{\text{isen}}}{\dot{W}_{\text{brake}}} = \frac{h_{\text{out,isen}} - h_{\text{in}}}{h_{\text{out}} - h_{\text{in}}} \tag{1}$$

DOI: 10.1002/er

Table I. Input data used for the microturbine modelling in Aspen Plus.

Constant parameters	Values
Inlet air composition	21% oxygen, 79% nitrogen
Compressor inlet pressure	1 bar
Compressor isentropic efficiency	74%
Compressor mechanical efficiency	89%
Compression ratio	3.35
Hot stream outlet temperature approach	93°C
Fuel composition	88% propane (C_3H_8) 12% *n*-butane (C_4H_{10})
Fuel pressure	3.35 bar
Turbine isentropic efficiency	86%
Turbine mechanical efficiency	97.4%
Turbine discharge pressure	1 bar

where $\dot{W}_{isen}$ is the power that would be delivered in isentropic compression and $\dot{W}_{brake}$ is the power delivered to the fluid. Therefore, $h_{out,isen}$ is the outlet enthalpy assuming isentropic compression, and h_{out} and h_{in} are the outlet and inlet compressor enthalpies, respectively. Typical isentropic efficiencies lie between 70 and 92% depending on the compressor type and compression ratio (Seider *et al.*, 1999). The following input parameters are also introduced:

— The temperature of the inlet air (T_1) in the compressor after it passes through the air filter and after cooling the electric generator. This is obtained from the experimental data in the first column of Table I.
— Inlet air pressure.
— The discharge pressure, set at 3.35 bar (Table I) in accordance with the pressure of the fuel supply system.
— Mechanical efficiency. This parameter, used to calculate the brake horsepower in the compressor, is defined as

$$\eta_{mech} = \frac{\dot{W}_{indicated}}{\dot{W}_{brake}} \tag{2}$$

where $\dot{W}_{indicated}$ is the total enthalpy change in the stream and $\dot{W}_{brake}$ is the total work of the compressor corrected for mechanical efficiency. The efficiencies for the compressor model are shown in Table I (input data). These data and those from other blocks were selected through several iterations and led to a good agreement with respect to the experimental results.

Regenerator: The regenerator is simulated using the *HEATX* block of Aspen Plus and the shortcut calculation type is selected with an average hot stream outlet temperature approach as the main specification set according to the experimental results.

Combustion chamber: The combustion chamber is simulated using a stoichiometric reactor (*RSTOIC* block). The following individual combustion reactions for propane and *n*-butane are used:

$$C_3H_8 + 5O_2 \rightarrow 3CO_2 + 4H_2O \tag{3}$$

$$C_4H_{10} + 6.5O_2 \rightarrow 4CO_2 + 5H_2O \tag{4}$$

DOI: 10.1002/er

The following stoichiometric balance of the fuel and air is used to calculate the theoretical air/fuel mass flow rate ratio for the propane/butane gaseous fuel:

$$0.88C_3H_8 + 0.12C_2H_{10} + 6.06O_2 + 22.72N_2 \Rightarrow 3.12CO_2 + 5.88H_2O + 22.78N_2 \quad (5)$$

The real air/fuel mass flow rate ratio is obtained by considering 600% excess air. The theoretical air/fuel mass flow rate ratio is therefore 18.3 kg air/kg fuel and the real air/fuel mass flow rate ratio is 128.1 kg air/kg fuel.

In the *RSTOIC* block, the following parameters are introduced:

— Fuel composition.
— Fuel pressure.
— Fuel temperature, taken as the ambient temperature, which varied in each case simulated.

Gas turbine: This is simulated using the isentropic efficiency to model the real turbine behaviour using the *COMPR* block of Aspen Plus. This is the same block as that used for the air compressor, but the isentropic efficiency is now defined as

$$\eta_{\text{isen}} = \frac{\dot{W}_{\text{break}}}{\dot{W}_{\text{isen}}} \quad (6)$$

As well as isentropic efficiency, the other input parameters required are:

— Mechanical efficiency defined as in the compressor model.
— The turbine discharge pressure.

As the exhaust gas temperature from the turbine is kept constant at 594 °C by the microturbine control, and as the model results have to reach the net output power obtained experimentally, two constraints were included in the simulation. Aspen Plus iteratively calculated these two fixed variables using a tool called 'Design specifications'. The first of these constraints is the exhaust gas temperature (T_6), which is set to the desired value of 594 °C (experimental value). The second constraint is the value of the net power, which is also obtained experimentally. The calculated value must be in agreement with the desired value (experimental value) within a given tolerance. The objective function relation is therefore

$$|\text{Desired value} - \text{Calculated value}| < \text{tol} \quad (7)$$

To reach the desired value, an input or manipulated variable must be selected and adjusted. The input variable used in the first constraint is the air mass flow (stream 1, Figure 1), for which an initial value is provided. The input variable used in the second constraint is the fuel mass flow rate (stream 4, Figure 1). Providing a good initial value of the manipulated variable helps to reach design specification convergence in a few iterations. The convergence method used was the secant linear approximation method, which is recommended by Aspen Plus for single design specifications. The value of the manipulated variable converges when the following statement is true:

$$\left|\frac{X_i - X_{i-1}}{X_{i-1}}\right| \leqslant \text{tol} \quad (8)$$

where X is the variable that should be converged, i the iteration number and tol the tolerance.

DOI: 10.1002/er

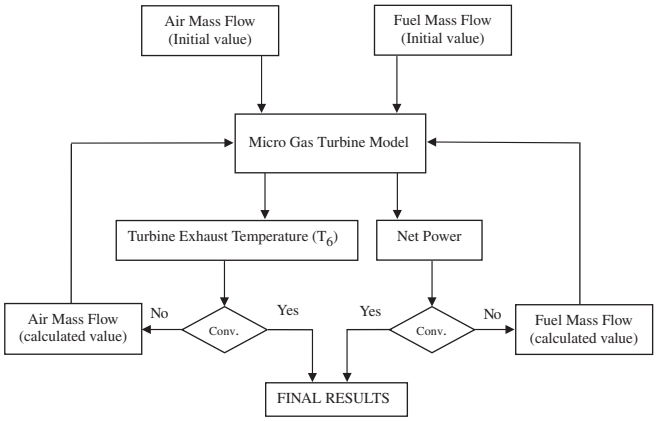

Figure 8. Flow diagram showing the model restrictions used to match the experimental data.

At the start of the simulation, X_{i-1} represent the suggested value and X_i represent the calculated value, as shown in Figure 8. The tolerance in our model was set at 0.001.

Also for the micro gas turbine model, an Excel spreadsheet is used to obtain in the report the net power produced by subtracting the power consumed by the compressor from the turbine power produced.

5. RESULTS

To obtain an empirical correlation for the microturbine net output power (Watts) as a function of the ambient temperature (°C), we selected experimental data from Figure 5, trying to collect the data from the zone with greater dot pitch at almost uniform intervals (~ 0.5°C). A sample of $n = 10$ values of net output power for each ambient temperature value was statistically evaluated to obtain the representative values shown in Figure 9. Also shown are the standard deviation of each representative value and the linear regression equation, which is represented as an empirical correlation by

$$\dot{W}_{\mathrm{no}} = 33\,100(\pm 2200) - 310(\pm 80)T_{\mathrm{a}} \tag{9}$$

The linear empirical correlation to obtain the net power output ($\dot{W}_{\mathrm{no}}$) is represented with the confidence limits (confidence level of 95%) on the intercept and slope, respectively. The confidence level of 95% is also applicable to Equations (10) and (12). Rounded off rules were applied to the numerical values on the correlations and these were statistically reported as in Andaverde *et al.* (2005).

The representative experimental data from net output power were entered into the simulation model to obtain the remaining operation variables. The numerical simulation provides further information about the operating conditions. Table II, for example, shows the temperatures for each stream in the microturbine. Temperature T_4, the fuel temperature, is assumed to be at ambient temperature. T_1 and T_6 (compressor inlet temperature and turbine outlet temperature) are experimental measurements and the rest are calculated values. As we mentioned before, the turbine exit temperature (T_6) is kept constant by the microturbine control system. Table II illustrates the increase in temperature of the exhaust gas to the recovery boiler (T_7) as the

DOI: 10.1002/er

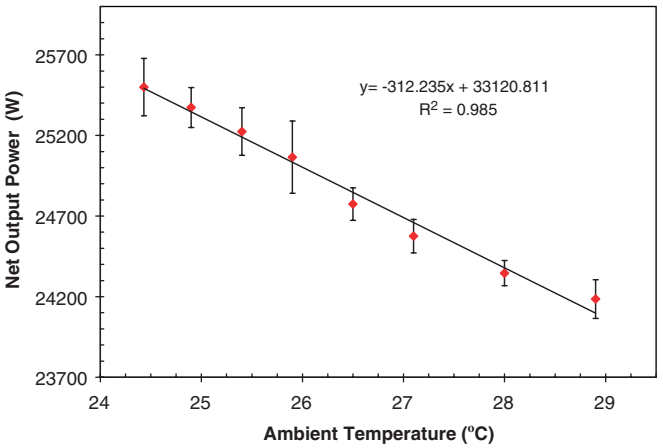

Figure 9. Representative experimental data of net output power from the micro gas turbine as a function of ambient temperature, used as input data for the micro gas turbine model and showed with the error bars (standard deviation) and linear regression equation.

Table II. Microturbine cycle temperatures for each stream according to Figure 1.

Ambient temp. (°C) (measured)	T_1 (°C) (measured)	T_2 (°C) (calculated)	T_3 (°C) (calculated)	T_4 (°C) (measured)	T_5 (°C) (calculated)	T_6 (°C) (measured)	T_7 (°C) (calculated)
24.4	32.7	201.0	513.9	24.4	842.8	594	294.0
24.9	32.5	201.0	514.0	24.9	842.8	594	294.0
25.4	32.0	201.2	513.9	25.4	842.8	594	294.2
25.9	33.0	201.8	513.9	25.9	842.8	593	294.8
26.5	34.5	202.8	513.9	26.5	842.8	594	295.8
27.1	34.3	203.7	513.9	27.1	842.8	593	296.7
28.0	35.3	205.3	513.8	28.0	842.8	594	298.3
28.9	34.9	204.7	513.8	28.9	842.8	594	297.7

ambient temperature increases. The temperature at the outlet of the combustion chamber (T_5) does not change. This is because of the constant air/fuel mass flow rate ratio and the almost negligible variation in the combustion chamber inlet temperatures (T_3).

Table III shows other important variables calculated with the simulation model. These results can be used to correlate the performance of the micro gas turbine with the ambient temperature and the fuel consumption required to produce a certain net power.

Fuel consumption is one of the outputs of the model but this variable was also measured during microturbine testing. Figure 10 compares the simulated and the experimental data for this variable and an empirical correlation, Equation (10), was obtained in order to determine the dependence of fuel consumption (kg/h) on ambient temperature (°C) with the microturbine working at its maximum full load.

$$\dot{m}_{\text{fuel}} = 10.13(\pm 0.26) - 0.065(\pm 0.010)T_{\text{a}} \tag{10}$$

To determine the correlation between the experimental and simulated values of fuel consumption, the linear correlation coefficient is obtained by the following expression

DOI: 10.1002/er

Table III. Main operating parameters for the microturbine cycle as a function of ambient temperature.

Ambient Temperature (°C) (measured)	Turbine output (kW) (calculated)	Compressor input (kW) (calculated)	Net power (kWe) (measured)	Fuel consumption (kW) (calculated)	Electrical efficiency (%) (calculated)
24.4	79.2	53.7	25.5	110.1	23.17
24.9	78.8	53.5	25.3	109.5	23.17
25.4	78.4	53.2	25.2	108.9	23.15
25.9	78.1	53.1	25.0	108.6	23.09
26.5	77.6	52.8	24.8	107.8	22.97
27.1	77.3	52.7	24.6	107.4	22.88
28.0	77.1	52.8	24.3	107.1	22.71
28.9	76.4	52.2	24.2	106.1	22.79

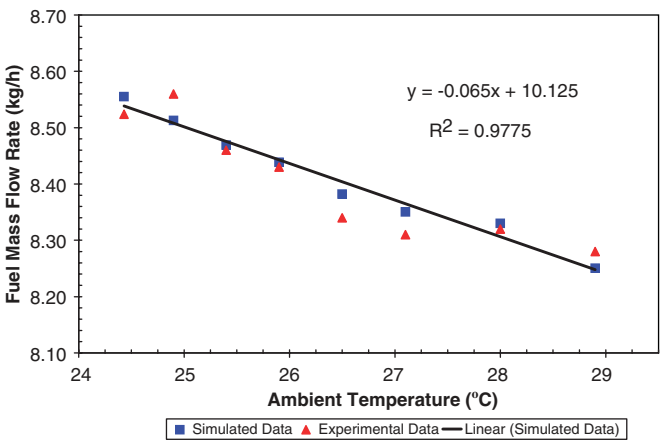

Figure 10. Microturbine fuel consumption for the simulated and the experimental data.

(Verma, 2005):

$$r = \frac{\sum_{i=1}^{n} \{(x_i - \bar{x})(yi - \bar{y})\}}{\sqrt{\{\sum_{i=1}^{n} (x_i - \bar{x})^2\}\{\sum_{i=1}^{n} (yi - \bar{y})^2\}}} \tag{11}$$

A value of $r = 0.953$ was obtained, which is greater than the critical value ($r = 0.707$) reported by Ebdon (1988) for a confidence level of 95%. There is therefore a good correlation between the data set.

The exhaust gas mass flow rate depends on the microturbine load and the ambient temperature. Figure 11 shows the calculated decrease in this flow with ambient temperature for the microturbine working at the maximum power allowed by the existing ambient temperature

$$\dot{m}_{\text{gas}} = 1195(\pm 31) - 7.7(\pm 1.2)T_{\text{a}} \tag{12}$$

The correlation represented by Equation (12) is very useful in the simulation and design of thermally driven energy systems, and can be is complemented with data of Table II to predict the thermal load that could be recovered of this gas stream.

DOI: 10.1002/er

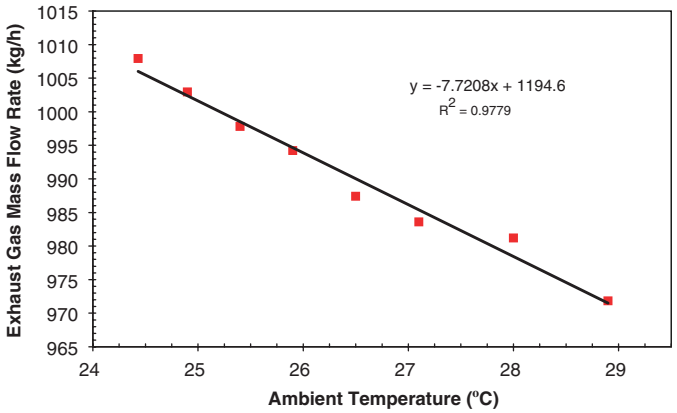

Figure 11. Calculated exhaust gas mass flow rate as a function of ambient temperature.

6. CONCLUSIONS

In this paper we have presented a modelling method for micro gas turbines to predict system performance. To obtain the model parameters and adjust some key variables, we used real data from the 30 kWe propane-driven microturbine of an experimental facility.

The model proposed in Aspen Plus includes the special functioning characteristics of a real microturbine, e.g. the increased air temperature due to the electric generator cooling and the minimum temperature allowed at the turbine outlet operating at maximum power load. This model is useful for obtaining the performance of the microturbine at the high temperatures found when microturbines are integrated with thermally activated cooling technologies during the high-temperature season. Empirical correlations were obtained to estimate the net power output power, the fuel consumption and the exhaust gas mass flow rate. Other useful parameters for the simulation and design of thermally driven energy systems, such as the exhaust gas temperature and electric efficiency, were calculated.

Our results show that an increase in the ambient temperature from 24.4 to 28.9 °C could produce a reduction in the exhaust gas flow to the directly fired chiller of around 5% and an increase in the exhaust temperature to the chiller of 7.5 °C.

In the range of temperatures studied, net power decreased by 5.1% and power efficiency decreased by 2.0%. All these results include the effect of the increased ambient air temperature due to the cooling of the electric generator by the combustion air before it is compressed by the air compressor.

NOMENCLATURE

AC = air compressor
CC = combustion chamber
COP = coefficient of performance
EG = electric generator
GT = gas turbine

DOI: 10.1002/er

h = specific enthalpy ($kJ\,kg^{-1}\,K^{-1}$)
LHV = lower heating value ($kJ\,kg^{-1}$)
MGT = micro gas turbine
n = number of measurements
r = correlation coefficient
RE = regenerator
T = temperature (°C)
TET = turbine exit temperature (°C)
tol = tolerance
$\dot{W}$ = power required or produced (W)
X = variable that should be converged in the simulation model
x = experimental values
$\bar{x}$ = arithmetic mean of n values of x
y = values obtained with the simulation model
$\bar{y}$ = arithmetic mean of n values of y

Greek letters

η = efficiency

Subscripts

a = ambient
i = iteration number/value of ith measurement
in = inlet
isen = isentropic
mech = mechanical
no = net outlet
out = outlet

ACKNOWLEDGEMENTS

We would like to acknowledge the contributions to the experimental part of the work made by Mr Jordi López and Mr Gerard Torres. Adrian Vidal would like to thank Posgrado de Ingeniería of UNAM for financing his short stay at CREVER in Tarragona, Spain. Dr Roberto Best would like to thank the Government of Catalonia for financing his sabbatical stay at CREVER. This work was partly supported in Mexico by CONACYT project U 44764-Y.

REFERENCES

Andaverde J, Verma SP, Santoyo E. 2005. Uncertainty estimates of static formation temperatures in boreholes and evaluation of regression models. *Geophysical Journal International* **160**:1112–1122.
Aspen Plus, Aplus 121. 2003. Physical property methods. User Guide, Chapter 7, Aspen Plus Product Documentation: Cambridge, Massachusetts, U.S.A.
Aspen Plus, version 12.1. 2004. Aspen Technology, Inc.: Cambridge, U.S.A., www.aspentech.com
Banetta S, Paganucci F, Giglioli R. 2001. System description and test planning for a combined heat and power (CHP) plant composed by a micro gas turbine and an absorption chiller/heater. *Proceedings of ASME Turbo Expo*, Louisiana, U.S.A.

DOI: 10.1002/er

Bouvy C, Koepsell M, Pfeiffer J. 2004. Evaluation of high temperature heat generation with micro-gas turbines. *10th International Symposium on Transport Phenomena and Dynamics of Rotating Machinery*, Honolulu, HI.
Broad Air Conditioning. 2005. http://www.broad.com.cn/english/product1.htm
Bruno JC, Massagués Ll, Coronas A. 2004. Stand-alone and grid-connected performance analysis of a regenerative micro gas turbine cogeneration plant. *Institution of Mechanical Engineers, Part A: Journal of Power and Energy* **218**:15–22.
Bruno JC, Valero A, Coronas A. 2005. Performance analysis of combined microgas turbines and gas fired water/LiBr absorption chillers with post-combustion. *Applied Thermal Engineering* **25**:87–99.
Bullin A. 2002. An introduction to micro turbine generators. In *Micro-Turbine Generators*, Chapter 1, Moore MJ (ed.). Professional Engineering Publishing: U.K.
Campanari S, Boncompagni L, Macchi E. 2002. Microturbines and trigeneration: optimization strategies and multiple engine configuration effects. *Proceedings of ASME Turbo Expo-GT-30417*, Amsterdam, Netherlands.
Capstone. 2001. *Capstone Microturbine Model 330—Installation and Start-Up*. Capstone: Chatsworth California, U.S.A.
Cowie M, Liao X, Radermacher R. 2003. Second generation integrated microturbine, absorption chiller and solid wheel desiccant system. *International Congress of Refrigeration*, ICR0331, Washington.
Ebdon D. 1988. *Statistic in Geography*. Basic Blackwell: Oxford.
Elliott Energy Systems. 2003. http://www.elliottmicroturbines.com/
Fairchild PD, Labinov SD, Zaltash A, Rizy DT. 2001. Experimental and theoretical study of microturbine-based BCHP system. *ASME International Congress*, New York, U.S.A. 11–16 November.
Gomes E, do Nascimento M, Lora E, Pilidis P, Haslam A. 2004. Performance evaluation and case studies of microturbines fuelled with natural gas and diesel. *Institution of Mechanical Engineers, Part A: Journal of Power and Energy* **218**:599–607.
Kren C, Schweigler C, Ziegler F. 2005. Heat transfer characteristics in flue gas fired regenerators of water/lithium bromide absorption chillers. *International Sorption Heat Pump Conference*, Denver, CO, U.S.A.
Ho JC, Chua KJ, Chou SK. 2004. Performance study of a microturbine system for cogeneration application. *Renewable Energy* **29**:1121–1133.
Hwang Y. 2004. Potential energy benefits of integrated refrigeration system with microturbine and absorption chiller. *International Journal of Refrigeration* **27**:816–829.
Invernizzi C, Iora P. 2005. Heat recovery from micro-gas turbine by vapour jet refrigeration systems. *Applied Thermal Engineering* **25**:1233–1246.
Pilavachi PA. 2002. Mini- and micro-gas turbines for combined heat and power. *Applied Thermal Engineering* **22**: 2003–2014.
Pinto C, Bazzo E. 2003. A thermoeconomic analysis of a small scale microturbine-absorption chiller cogeneration plant. *Proceedings of ECOS*, Copenhagen, Denmark; 177–185.
Sang E, Park C, Jeong S. 2005. Performance characteristics of exhaust gas heat exchangers for absorption chillers. *International Sorption Heat Pump Conference*, Denver, CO, U.S.A.
Seider WD, Seader JD, Lewin DR. 1999. *Process Design Principles: Synthesis, Analysis and Evaluation*. Wiley: New York.
UTC Power. 2005. http://www.utcfuelcells.com/utcpower/products/purecomfort.shtm
Verma SP. 2005. Estadística básica para el manejo de datos experimentales: Aplicación en la Geoquímica (Geoquimiometría). Universidad Nacional Autónoma de México, México, D.F.
Wang W, Cai R, Zhang N. 2004. General characteristics of single shaft microturbine set at variable speed operation and its optimization. *Applied Thermal Engineering* **24**:1851–1863.
Zhang N, Cai R. 2002. Analytical solutions and typical characteristics of part-load performances of single shaft gas turbine and its cogeneration. *Energy Conversion and Management* **43**:1323–1337.

DOI: 10.1002/er